

Figure 2 – Radiant positions of the showers listed in Table 1. ‘Aqr’ is the average of NDA, SIA, and NIA. Note the ‘jump’ between DCA and VIR (February 01) and again between VIR and SAG (April 15).

form this complex — the Taurids — is discussed below. Other showers can hardly be distinguished from the sporadic background but were part of radiant searches in the past with the result of numerous minor showers in the vicinity of the ecliptic. The centers of these radiants are used in the current working list.

For various reasons, the centers of the radiant area as used in the current working list of meteor showers and in numerous publications are not continuously moving along the ecliptic throughout the year. One historic reason is that the last working list was established with the intention of keeping the known radiants and shower designations such as Virginids etc. This fit causes some

Table 1 – Ecliptical meteor showers which are now subsumed as the antihelion source.

Ecliptical shower	Abbreviation	Activity period
$\delta$ -Cancrids	DCA	Jan 01–Jan 31
Virginids	VIR	Feb 01–Apr 15
Sagittarids	SAG	Apr 15–Jul 00
Northern $\delta$ -Aquadrids	NDA	Jul 15–Aug 25
Southern $\iota$ -Aquadrids	SIA	Jul 15–Aug 25
Northern $\iota$ -Aquadrids	NIA	Aug 11–Aug 31
Piscids	SPI	Sep 01–Oct 01
Northern and Southern Taurids	NTA, STA	Oct 01–Nov 25
Northern $\chi$ -Orionids	XOR	Nov 25–Dec 15

inconsistencies which become most obvious at the times of transition between two successive ecliptical showers. This is clearly visible in Figure 2.

Recent radar observations suggest that the center should be close to  $12^\circ$  east of the antihelion direction with no specific deviation over the year. This complex will be named antihelion source for the VMDB data storage from 2007 onwards (Arlt & Rendtel, 2006). In the past the antihelion data is subsumed as a sequence of ecliptical showers listed in Table 1.

Detailed information about the inclusion and exclusion of certain showers, especially in the summer period, is discussed by Arlt & Rendtel (2006). In the present analysis of sporadic meteor activity the summary of showers as listed in Table 1 was used to represent the antihelion source. The northern and southern branches of the Taurids were summarized as the Taurids for this study.

## 2.2 Rate variations of the antihelion source

First, we need to know the variation of the population index  $r$ . Here we may use the values found from the analysis of the listed ecliptical showers. In fact, the values differ only little from  $r = 3.0$ , except for the Taurid period where  $r = 2.5$  was used. Hence we used  $r = 3.0$  for all periods except the interval from October 1 until November 25. With this figure we were able to

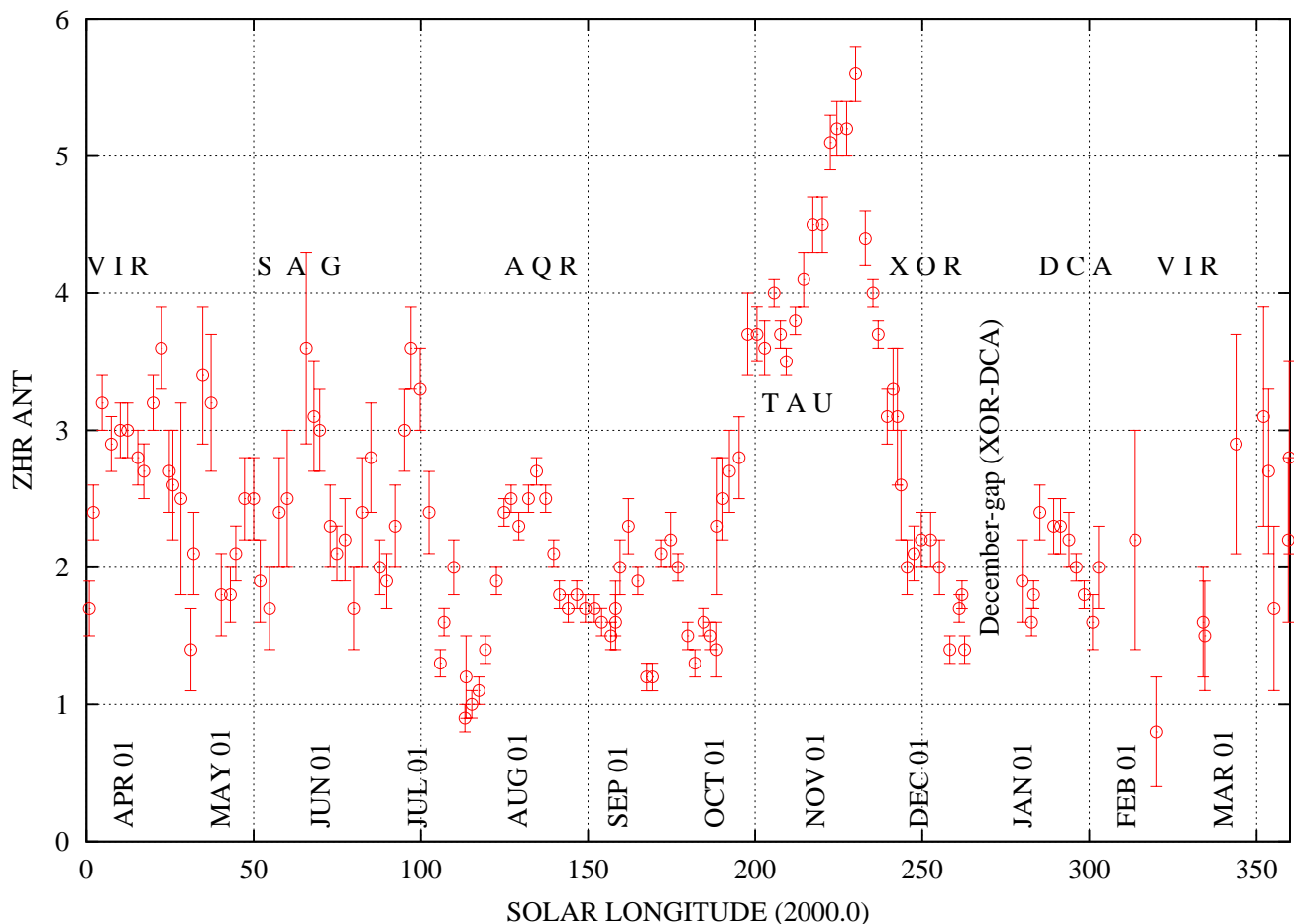


Figure 3 – ZHR of the showers now summarized as antihelion source based on visual data observed between 1984 and 2005.

calculate the ZHR of the entire series of showers from the antihelion region.

It is known that the accuracy of visual meteor observations suffers from errors of the shower association. While the effect is negligible for major showers in the vicinity of their peaks, all minor sources are affected. This is considered by the assumption of a radiant area rather than a point. Its size should compensate the loss of true shower members and non-shower meteors erroneously associated with the radiant. Close to the peaks of major showers observers apply the counting method so that a careful check of the shower association as in the periods of generally low activity is not possible. This does not harm the major shower's data, but the lost shower meteors now classified as sporadic do change both the numbers and the magnitude distribution (as most showers have a lower value of  $r$  around their peaks). For an analysis of the antihelion ZHRs shown in Figure 3 we therefore omitted the immediate major shower peak periods (Quadrantids, Perseids, Leonids, Geminids). The effect was found to be largest near the Leonid peaks with their exceptional ZHRs in the years between 1998 and 2002.

Except for the Taurids, there is no significant rate enhancement visible. This may be due to unresolvable structures in the antihelion region, but radar data show a similar scatter (Campbell-Brown & Jones, 2006). For the  $\delta$ -Cancriids and the Aquarid period a profile with a

maximum occurs. This could be an artefact as the position of the 'true' antihelion source moves through the assumed ecliptical shower radiant and thus increasing the number of meteors fitting the assumed radiant position. But it is also possible that there is indeed some structure in the antihelion meteoroid orbit distribution which led to the definition of the ecliptical showers in the past. This is not unlikely, as the majority of orbits of sporadic (antihelion) meteors is associated with comet 2P/Encke (Štohl, 1987), and there is a large number of similar objects which are possible or established parent objects for minor streams. A third possibility cannot be ruled out: an observer's bias 'supporting' a shower association in the vicinity of a predicted maximum.

The annual average ZHR from the antihelion region amounts to approximately 2.5 (using  $r = 3.0$ ). The Taurids being exceptional with a ZHR up to 5.3 ( $r = 2.5$ ).

The shapes of the rate and flux profiles between the visual data analysed here and the radar fluxes as shown in (Campbell-Brown & Jones, 2006) are not identical. However, we have to bear in mind that the radar fluxes consider meteors typically of magnitude +8 while the visual meteors represent mainly the magnitudes +3 or +4 and hence a different mass range. This may also explain the lack of a Taurid maximum in the radar flux data (Campbell-Brown & Jones, 2006).

### 3 Apex source

#### 3.1 Data sample

A visual meteor observer checks whether a seen meteor fits any radiant position (plus length and angular velocity) of the working list. The remaining meteors are classified as sporadic with no further distinction. Therefore meteors stored as ‘SPO’ in the VMDB files include those from the region around the apex of the Earth’s orbital motion (abbreviated to apex here), the toroidal sources and those moving on other orbits including minor, unresolved sources. The composition of the SPO-sample will of course vary in the course of the night. In particular, meteors of the apex region will dominate towards the morning, while the toroidal meteors should contribute with a rather constant amount over the entire night. Contributions from other sources are likely very small as they are not explicitly identified as radiants.

Using all meteor trails plotted or recorded by video meteor cameras, one can search for a ‘radiant’ among the sporadic meteors. Accepting a range of velocities between 40 and 70 km/s as found from radar data (Jones & Brown, 1993) does not show any significant hint on a radiant in the apex region. Obviously, the radiant area is extremely smeared over the region in the sky. The main reason, however, may be the nature of this activity. It is caused by meteoroids on almost retrograde orbits. Their movement is superposed by the Earth’s motion which leads to a focusing effect. Consequently, it is not a real source like a stream originating from a parent, but rather an effect of the relative motion of the meteoroids and the Earth.

#### 3.2 Population index

First, we need to know the variation of the population index of the meteors labelled ‘SPO’. The assumed standard value is  $r = 3.0$ . The sample collected as SPO is not completely identical with the apex meteors outlined before as it includes pre-midnight non-apex meteors.

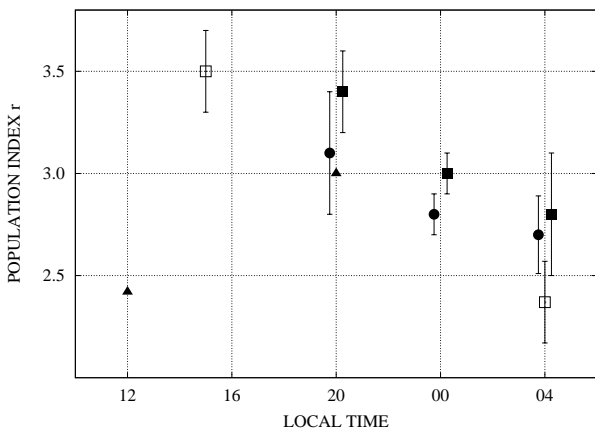


Figure 4 – Diurnal variation of the population index  $r$  of sporadic meteors from the VMDB data in February (filled squares) and October (filled circles). These points actually occur exactly on the hour, but are offset sideways slightly for visibility. Other values are from radar data (Babadzhanov & Bibarsov, 1992) (triangles) and from optical data (Hughes & Stephenson, 1972) (open squares).

Generally, the value of  $r$  is higher in the evening sector (around 18<sup>h</sup> local time) and decreases towards dawn (Figure 4). If we assume that the mass distribution is almost identical among all sources of sporadic meteoroids (as explained at the beginning), the larger number of high-velocity retrograde meteors towards the morning may account for this effect.

However, the expected differences by mixing other than the apex meteors into the sample are smaller than the scatter found in the individual intervals. The result shown in Figure 5 has already been published by Rendtel (2004). The annual average value is  $r = 2.95 \pm 0.15$ . Not surprisingly, this general value is quite similar to the one found for the antihelion meteors. Variations may occur at a seasonal scale as well as in shorter periods, as discussed by Rendtel (2004). However, the data is not sufficient to test whether these are  $r$ -variations indeed recur at fixed positions (which could hint at some persistent structures among the apex meteoroids) or just random variations.

#### 3.3 Apex rate

The standard procedure to calculate a rate of sporadic meteors includes a value of  $r = 3.0$  and no radiant position. This gives a ‘global’ hourly rate only corrected for the limiting magnitude of 6.5. Recall that calculating a true ZHR from raw data includes a correction for the zenith angle of the radiant. However, we may determine a rough estimate for the ZHR of the apex source if we assume the position which is obtained by the radar data (Campbell-Brown & Jones, 2006). In fact, this will mainly include data obtained after local midnight when the apex region appears above the horizon. This allows to combine data from different locations as in normal meteor shower analyses. We may account for the rate caused by other sources by subtracting a constant value but, as already pointed out, the contribution of the toroidal and other minor showers is negligible. This way we should be able to follow the number density in the apex region including the possibility of detecting intervals with higher spatial particle densities if these exist at all.

We now calculate the ZHR of the sporadic meteors using a value of  $r = 2.95$  and the northern apex position as found by Campbell-Brown & Jones (2006).

Again, we find increased ZHRs during the activity of a few major showers. Not surprisingly, the  $\eta$ -Aquarids seem to cause enhanced sporadic (apex) rates with their radiant close to the apex. The effect during the Perseids and the Geminids may be of more general nature, i.e. shower meteors not correctly associated increase the number of meteors noted as ‘SPO’ in the visual data. Some further shower maxima are indicated in Figure 6. There is no such obvious increase of the rate during the Quadrantids and the Orionids, for example. The annual average ZHR of the apex source is 22 with higher ZHRs (exceeding 25) in August and September as well as end-January and lowest ZHRs in June — again supposing that there is no systematic effect from the toroidal source superposed on the rates.

As in the case of the antihelion source, we see dif-

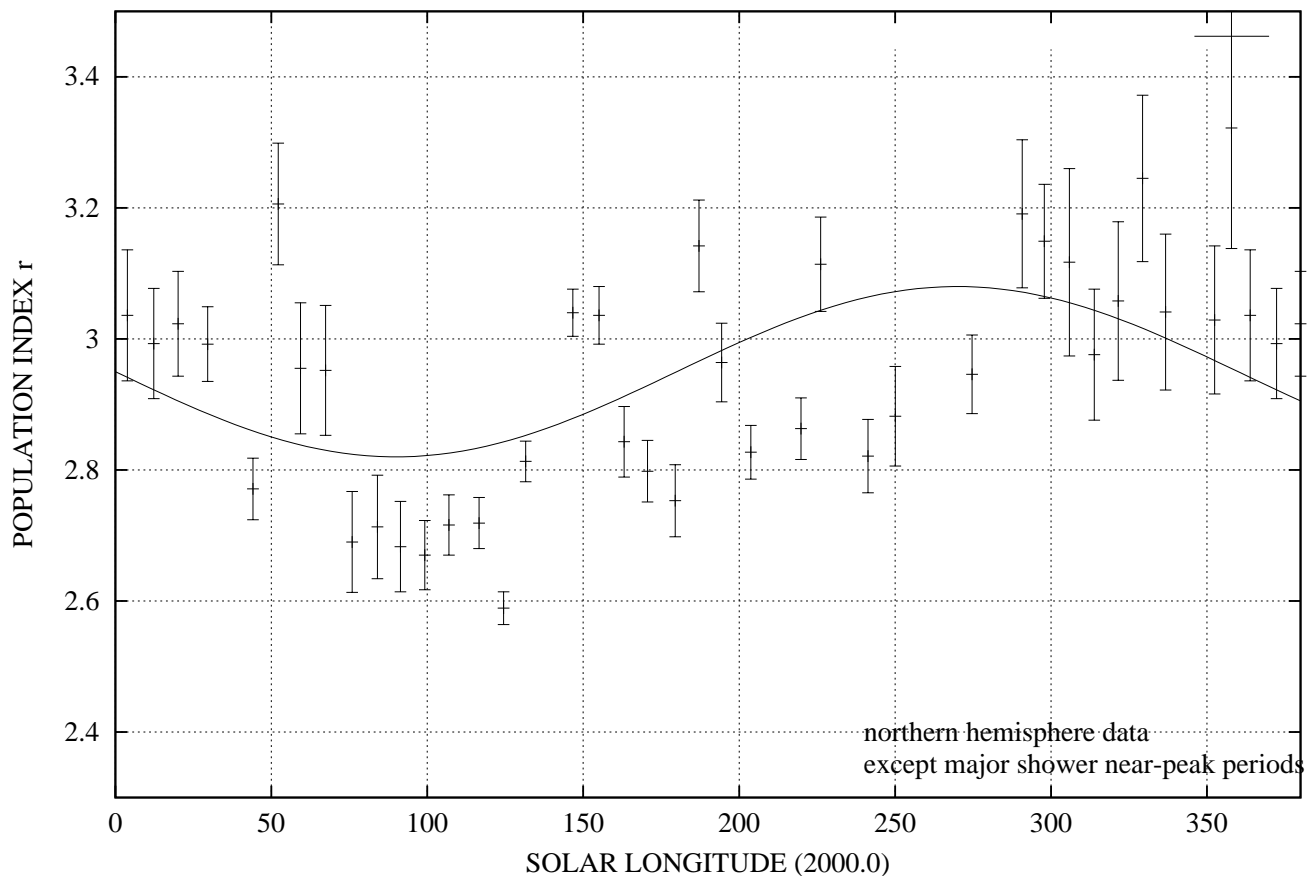


Figure 5 – Population index  $r$  of meteors labelled as ‘SPO’ in the VMDB. The sample includes visual data from the northern hemisphere collected between 1988 and 2003 and excludes the near-peak periods of major showers. The curve is an attempt to fit the annual variation with a sinusoid independent of whether this is appropriate to the particle distribution along the Earth’s orbit. The general shape does not correlate with the declination of the apex region and thus hints at other reasons for its variation.

ferences between the radar flux as found by (Campbell-Brown & Jones, 2006) and the visual ZHRs which certainly are determined by the different particle populations contributing to the samples. Notably, there are coinciding features of the radar flux and visual ZHR, i.e. a minimum around  $\lambda_{\odot} = 85^{\circ}$  in June and maxima around  $\lambda_{\odot} = 150^{\circ}$  (second half of August until September) as well as  $\lambda_{\odot} = 290 - 300^{\circ}$  (January/February). In a next step we try to find out whether the features in the profiles are stable and present in subsets of the sample. The time covered by the data collection (1984–2006) should be sufficient for this purpose.

#### 4 Conclusions

The analysis of the activity from the antihelion source leads to the replacement of a series of apparently independent ecliptical showers by one continuous source with the exception of the Taurid period. This is introduced in the new working list of meteor showers published by Arlt & Rendtel (2006). This antihelion source continues throughout the year and hence provides a radiant in Gemini in the second half of December. This period virtually had no ecliptical radiant in the previous list.

Although there is no explicit information about meteors associated with the apex region stored in the VMDB, it is possible to calculate the population index

$r$  and a ZHR for these meteors summarized as sporadic (SPO). Contrary to the antihelion source, which is associated with short-period comets and minor planets, the apex source is merely a focussing effect of almost retrograde meteoroid orbits. We find an annual average of  $r = 2.95 \pm 0.15$  with a minimum near  $\lambda_{\odot} = 80^{\circ}$  (June) and a maximum near  $\lambda_{\odot} = 270^{\circ}$  (end of the year). The ZHR of the northern apex region yields enhanced values at the peaks of three showers, the  $\eta$ -Aquadrids, the Perseids, and the Geminids. Structures in the rate profile may exist. We find significant differences between the radar flux profiles (Campbell-Brown & Jones, 2006) and the visual data which have to be attributed to the different magnitude ranges covered by the two methods. Some coinciding features of the radar flux and visual ZHR can be found: a minimum near  $\lambda_{\odot} = 85^{\circ}$  in June and maxima around  $\lambda_{\odot} = 150^{\circ}$  (second half of August until September) and  $\lambda_{\odot} = 290 - 300^{\circ}$  (January/February).

#### References

- Arlt R. and Rendtel J. (2006). “A new working list of meteor showers”. *WGN*, **34:3**, 77–84.
- Babadzhanov P. B. and Bibarsov R. S. (1992). “The mass distribution of sporadic meteoroids — Results of radar observations of overdense meteor trails”. *Astronomicheskii Vestnik*, **2**, 103–108. In Russian.

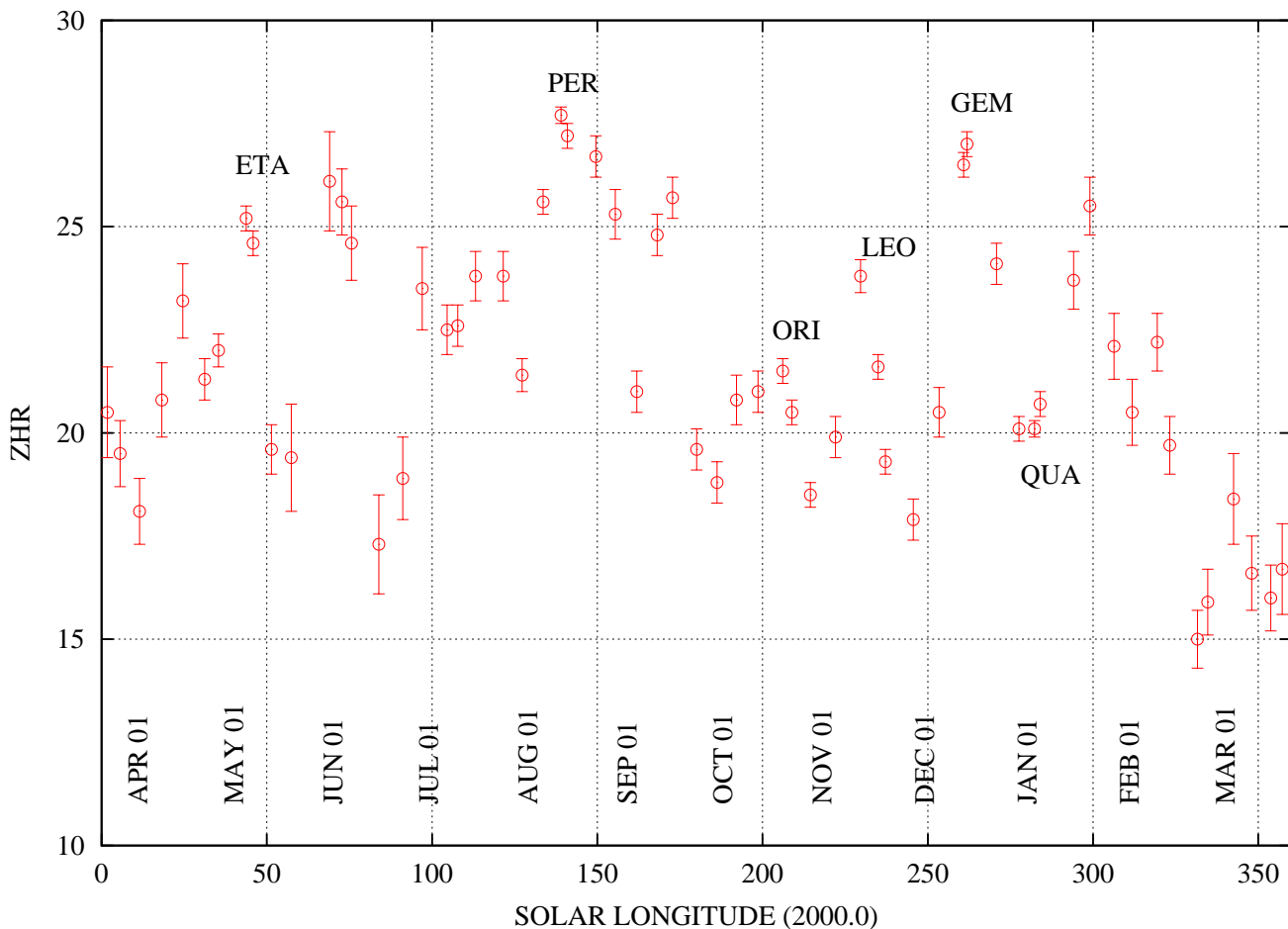


Figure 6 – ZHR of the meteors labelled as ‘SPO’ in the VMDB, which are representative of the activity of the north apex source. The sample includes visual data from 1984 to 2005. Peaks of some showers are marked, with ETA, PER and GEM obviously ‘polluting’ the SPO sample.

Campbell-Brown M. D. and Jones J. (2006). “Annual variation of sporadic meteor rates”. *MNRAS*, **367**, 709–716.

Hughes D. W. and Stephenson D. G. (1972). “The diurnal variation in the mass distribution of sporadic meteors”. *MNRAS*, **155**, 403–413.

Jones J. and Brown P. (1993). “Sporadic meteor radiant distributions: orbital survey results”. *MNRAS*, **265**, 524–532.

Rendtel J. (2004). “The population index of sporadic meteors”. In *Proceedings of the International Meteor Conference, Bollmannsrub, Germany, September 19-21, 2003*, pages 114–122. International Meteor Organization, Potsdam.

Štohl J. (1987). “Meteor contribution by short period comets”. *A&A*, **187**, 933–934.